



## ISTITUTO NAZIONALE DI RICERCA METROLOGICA Repository Istituzionale

Exploring the potential of Raman spectroscopy for the identification of silicone oil residue and wear scar characterization for the assessment of tribofilm functionality

This is the author's submitted version of the contribution published as:

*Original*

Exploring the potential of Raman spectroscopy for the identification of silicone oil residue and wear scar characterization for the assessment of tribofilm functionality / Österle, W.; Giovannozzi, A.; Gradt, T.; Häusler, I.; Rossi, A.; Wetzel, B.; Zhang, G.; Dmitriev, A. I.. - In: TRIBOLOGY INTERNATIONAL. - ISSN 0301-679X. - 90:(2015), pp. 481-490. [10.1016/j.triboint.2015.04.046]

*Availability:*

This version is available at: 11696/57287 since: 2021-03-09T19:12:56Z

*Publisher:*

Elsevier

*Published*

DOI:10.1016/j.triboint.2015.04.046

*Terms of use:*

This article is made available under terms and conditions as specified in the corresponding bibliographic description in the repository

*Publisher copyright*

(Article begins on next page)

Manuscript Number: TRIBINT-D-15-00154R1

Title: Exploring the potential of Raman Spectroscopy for the identification of silicone oil residue and wear scar characterization for the assessment of tribofilm functionality

Article Type: Full Length Article

Keywords: Raman spectroscopy,  
Cross-sectional TEM,  
Silicone oil residue,  
Tribofilm

Corresponding Author: Dr. Werner Oesterle,

Corresponding Author's Institution: Federal Institute for Materials Research and Testing

First Author: Werner Oesterle

Order of Authors: Werner Oesterle; Andrea Giovannozzi; Thomas Gradt; Ines Haeusler; Andrea Rossi; Bernd Wetzel; Ga Zhang; Andrey I Dmitriev

Abstract: We applied a combination of Raman spectroscopy (RS) and cross-sectional transmission electron microscopy (X-TEM) to identify silicone oil residues and tribofilms at steel disc surfaces after tribological testing. Neither chemical cleaning nor mechanical removal of a 50 µm thick surface layer produced a surface without any silicone residue. Nevertheless, long-term tribological properties are not affected due to silicone degradation which has been proved by Raman spectroscopy. Excellent antiwear and antifriction properties of a nanocomposite at severe stressing conditions correlated with the formation of a silica-based tribofilm containing amorphous and graphite-like carbon nanoparticles. Since reliable carbon quantification by analytical TEM is difficult, RS is a useful complementary method for carbon identification at wear scars.

## Highlights

- Potential of RS for the identification of silicone oil residues proven
- Long-term tribological properties not affected by silicone oil residue
- Complementary results from different analytical techniques (RS, XTEM) beneficial for wear scar analysis

# Exploring the potential of Raman Spectroscopy for the identification of silicone oil residue and wear scar characterization for the assessment of tribofilm functionality

W.Österle<sup>a\*</sup>, A. Giovannozzi<sup>b</sup>, T. Gradt<sup>a</sup>, I. Häusler<sup>a</sup>, A. Rossi<sup>b</sup>, B. Wetzel<sup>c</sup>, G. Zhang<sup>c, d</sup>, A.I. Dmitriev<sup>e, f</sup>

<sup>a</sup> BAM Federal Institute for Materials Research and Testing, 12200 Berlin, Germany

<sup>b</sup> INRIM National Institute of Metrology Research, 10135 Torino, Italy

<sup>c</sup> IVW Institute of Composite Materials, University Kaiserslautern, 67663 Kaiserslautern, Germany

<sup>d</sup> State Key Laboratory of Solid Lubrication, Lanzhou Institute of Chemical Physics, Chinese Academy of Sciences, China

<sup>e</sup>ISPMS Institute of Strength Physics and Material Science SB RAS, 634021 Tomsk, Russia

<sup>f</sup>Tomsk State University, 634021 Tomsk, Russia

\* Corresponding author, E-mail: Werner.oesterle@bam.de

## Abstract

We applied a combination of Raman spectroscopy (RS) and cross-sectional transmission electron microscopy (X-TEM) to identify silicone oil residues and tribofilms at steel disc surfaces after tribological testing. Neither chemical cleaning nor mechanical removal of a 50 µm thick surface layer produced a surface without any silicone residue. Nevertheless, long-term tribological properties are not affected due to silicone degradation which has been proved by Raman spectroscopy. Excellent antiwear and antifriction properties of a nanocomposite at severe stressing conditions correlated with the formation of a silica-based tribofilm containing amorphous and graphite-like carbon nanoparticles. Since reliable carbon quantification by analytical TEM is difficult, RS is a useful complementary method for carbon identification at wear scars.

**Keywords:** Raman spectroscopy, Cross-sectional TEM, Silicone oil residue, Tribofilm

## 1. Introduction

Martensitic steel grade 100Cr6, corresponding to AISI 52100, is widely used for ball bearing applications. Discs made of 100Cr6 are widely used as counterbodies for all kinds of polymer matrix composites (PMCs) by the present authors [1-18] and others as well. The steel discs are usually supplied with a grinded surface providing an average surface roughness of  $R_a = 0.3 \mu\text{m}$ . Furthermore, manufacturers usually treat disc surfaces with silicone oil as a measure for preventing corrosion. It is important to remove the silicone oil from the disc surface prior to tribological testing against the friction or anti-friction materials being studied. The standard cleaning procedure is immersion in acetone, wrapping with acetone-soaked paper and rinsing with isopropanol. A study described in [4] has shown that this procedure leads to the same tribological behaviour as mechanical removal of a surface layer by grinding. Despite that, we observed an indication of silicone oil residue by analytical TEM while investigating a thin lamella prepared from a wear scar of a disc which was previously cleaned with acetone. Since it is very difficult to distinguish a silicon oil film from a tribofilm formed by rubbing a hybrid composite (containing silica nanoparticles) against the steel disc, it was important to eliminate silicone oil residues as extensively as possible. Therefore, we searched for a method having the capability to indicate even small amounts of silicone oil within an area of interest at the disc surface. As will be shown in the following, Raman spectroscopy (RS) is the method of choice. Other methods such as scanning electron microscopy (SEM) combined with energy dispersive x-ray spectroscopy (EDS) and cross-sectional transmission electron microscopy (X-TEM) confirmed and supplemented the RS findings. Finally, the impact of different cleaning procedures on the evolution of the coefficient of friction (COF) during pin-on-disc tests was studied.

Besides the motivation explained above, another issue was triggering the present study. It was a discussion about the coefficient of friction expected for the sliding of steel against steel. Our

experience with pins and discs of ferritic-pearlitic steel sliding against each other proves the evolution of a high COF in the range 0.7-0.8 after a short running-in period of lower friction [19]. This finding was confirming results found in literature [20, 21]. A reasonable explanation is that the formation of fresh metallic surfaces by wear provides the high COF. Other work from the literature considering mainly wheel-rail contact, suggest a lower COF in the range 0.3-0.55 under dry conditions [22, 23]. On the other hand, a literature review presented in Fig.4 of [23] suggested a COF in the range of 0.4 – 0.7 for dry friction of rails, depending on testing conditions. Furthermore, slight modifications of the surface which may be caused by the presence of water or organic material (leaves) on rails can change the COF drastically [23]. It is well known since tribology has become a scientific discipline that the COF is a system property and not merely a material property [24]. Therefore, chemical reactions occurring at the surfaces or retention of organic residues have to be taken into account when considering COF-evolution during tribological tests.

Finally, the third objective of this study was to supplement our knowledge on the structure of beneficial tribofilms formed during pin-on-disc tests of hybrid polymer matrix composites (PMCs) at high pv-values [1-3]. Previous studies with SEM/EDS [5] and TEM/EDS [4] revealed the importance of silica nanoparticles (SNPs) for film formation, but the extent to which carbonaceous species contribute to tribofilm structure and functionality were not scrutinized. Therefore, we applied Raman spectroscopy as additional method because of its high sensitivity towards both polymer and carbonaceous materials.

## **2. Experimental Procedure**

### **2.1 Materials**

INA (Schaeffler group, Germany supplied the 100Cr6 steel discs used in this study. The manufacturer treated the original discs with silicone oil. Material data and specifications of the oil are unknown to us. One disc was investigated in the as received condition, whereas the

other ones were cleaned with acetone and some of them also with toluene. Furthermore, some of the cleaned discs were subsequently ground with abrasive paper thus removing a surface layer of approximately 50  $\mu\text{m}$  from each side. While applying an automatic grinding machine (ATM Saphir 500) the procedure was the following: i) coarse grinding with SiC paper grade P260 with an applied force of 40 N for 2- 4 min. The removed layer was measured every 30 s with the aid of a micrometer gauge. ii) Fine grinding first with P400 and then with P600 paper with an applied force of 30 N for 30 s each. iii) Cross grinding with P600 paper and very low applied force in order to produce visible scratches in 4 directions at angles of 45°. Finally, we measured the surface roughness with the aid of white light profilometry and adjusted  $R_a$  to 0.3  $\mu\text{m}$  by eventually repeating step iii) several times. By applying this procedure, a similar topography as known from the original disc was obtained.

100Cr6 pins were also used as counter bodies for tribological testing. Furthermore, we performed two tests with hybrid composite pins. The latter material consists of an epoxy (EP) matrix with 10 vol.% of short carbon fibres (SCF), 8 vol.% graphite and 5 vol.% silica nanoparticles (SNP). A previously published paper described the tribological properties of this material [3]. Since only acetone-cleaned discs were considered during this previous study, we repeated the tests with freshly ground discs. Although, first results of this comparison were already presented in a separate paper [4], we have decided to discuss them here once more in the context of new findings. The following materials acted as reference materials for taking “fingerprint” Raman spectra: SiO<sub>2</sub> nanopowder (Sigma Aldrich, Taufkirchen, Germany), pure epoxy (IVW, Kaiserslautern, Germany) and the original 100Cr6 discs treated with silicone oil by the manufacturer (INA, Schaeffler group, Germany).

## **2.2 Raman spectroscopy**

Raman spectra were recorded using a Thermo Scientific DXR Raman equipped with a microscope, an excitation laser source at 532 nm, a motorized stage sample holder, and a

charge-coupled device (CCD) detector. Spectra of reference samples were collected using a 50x long working distance microscope objective with a 1 mW laser power and a spectral range from 3500 to 50  $\text{cm}^{-1}$  with a grating resolution of 5  $\text{cm}^{-1}$ . The acquisition time was 200 s with 1 s exposure time. Raman mapping on the surface of the steel discs was performed using a 100x microscope objective with a 1 mW laser power, a 1  $\mu\text{m}$  step size and a spectral range from 3500 to 50  $\text{cm}^{-1}$  with a grating resolution of 5  $\text{cm}^{-1}$ . The acquisition time was 100 s with 1 s exposure time for each spectrum of the map.

### **2.3 Electron microscopy**

A DualBeam FIB/SEM instrument (FEI Quanta 3D) equipped with an energy dispersive spectrometer (EDS) (EDAX Apollo XL) helped to identify regions of interest at the disc surfaces. Furthermore, the FIB instrument was used for target preparation of micron-sized cross-sectional lamella (100 nm thick) for further studies with the analytical transmission electron microscope (TEM). This special characterization technique using FIB-prepared cross-sections of surface films will be termed X-TEM in the following. An analytical TEM of type JEM 2200FS (JEOL) operated at 200 kV and equipped with EDS and an in-column energy filter was used for this purpose.

### **2.4 Tribological testing**

Pin-on-disc tests were performed with 100Cr6 pins rubbing against 100Cr6 discs for three different surface conditions: i) as received, ii) cleaned with acetone and iii) acetone-cleaned and additionally ground with abrasive paper.

As described in [21], a classical pin-on-disc tribometer of type WAZAU-SST with a maximum applicable load of 2000 N and maximum speed of 3000 revolutions per minute served well. A rotating pin is pressed against a stationary disc which is fixed on a support. A



spring applies the normal force which shifts the support in upward direction. A screw that can be manually accurately set defines the spring's tension.

The pin was 17 mm long and 5 mm in diameter with a slight spherical curvature corresponding to a radius of 50 mm and a rounding of the head's edges corresponding to a radius of 1 mm, in order to avoid difficulties with misalignment. Furthermore, surface roughness of the pin's head was similar to that of the disc surface (approximately  $R_a=0.3\text{ }\mu\text{m}$ ).

The following test parameters were used: Normal load  $F_N = 20\text{ N}$  and sliding velocity  $v = 0.05\text{ m/s}$ . The experiments lasted normally for 1 hour at ambient conditions, 20-25° C. Humidity was not controlled, but usually amounts to 50% inside the air-conditioned laboratory. Normal and friction forces were monitored during each test by means of LabView software. With a sampling rate of 20 Hz, one data point was obtained every 0.04 s, which resulted in about 80,000 data points per experiment. The data was analysed using Origin software. Graphs were smoothed with a 4500 or 2000 points moving average to emphasize the friction trend.

As described in [4], a similar series of experiments was performed with pins made of a conventional and a hybrid polymer matrix composite rubbing against 100Cr6 discs. Here two surface states were compared, namely after standard cleaning with acetone and removal of surface layers by dry grinding with SiC paper.

Table 1 provides an overview of the different testing conditions, mating materials and corresponding characterization results.

### **3. Results and discussion**

#### **3.1 Reference spectra**

The first series of RS-measurements had the objective to check the capability of the method to identify species of interest and to obtain their characteristic spectra (fingerprints). Figures 1a

and b show that both, silicone oil and epoxy resin produce strong Raman signals, and that the peaks of both species do not overlap, but provide characteristic fingerprints.

In particular, silicone oil fingerprint is mainly characterized by two sharp bands in the range  $1200\text{--}1000\text{ cm}^{-1}$  that are assigned to the Si–O–C and to the Si–O–Si stretching vibrations, whose intensity usually depends on the Si–O chain length [25]. Raman spectrum of silicone oil (Fig.1a) also exhibits typical stretching and bending vibration bands of  $\text{CH}_x$  aliphatic groups at  $3000\text{--}2800\text{ cm}^{-1}$  and at  $1600\text{--}1300\text{ cm}^{-1}$ , respectively.

Fig.1b shows the fingerprint of epoxy resin. Raman bands corresponding to epoxide vibration are in the range of  $1280\text{ cm}^{-1}$  and  $1230\text{ cm}^{-1}$  according to [26], here the epoxide vibration band is at  $1250\text{ cm}^{-1}$  (breathing of the epoxide ring). The peak at  $916\text{ cm}^{-1}$ , assigned to the epoxide ring deformation, is much weaker. Other Raman peaks at  $1108\text{ cm}^{-1}$ ,  $1180\text{ cm}^{-1}$  and  $1460\text{ cm}^{-1}$  belong to resin backbone vibrations [27]. Moreover,  $\text{CH}_x$  vibration bands over the  $3000\text{ cm}^{-1}$  suggest the presence of aromatic groups which is also confirmed by a double peak around  $1600\text{ cm}^{-1}$  which is assigned to C=C vibration of the aromatic ring.

The amorphous silica nanoparticles, although present in high quantity in form of dry powder particles, show only weak Raman signals (Fig.1c). The higher peak at about  $440\text{ cm}^{-1}$  corresponds to the R band ( $\omega\text{R}$ ) which is mainly generated by the oxygen atom bending in the Si–O–Si linkages [28]. Other peaks visible in the Raman spectrum are related to the D1 (breathing vibration mode of the 4-member rings) and D2 (breathing vibration mode of the 3-member ring) bands at  $490$  and  $600\text{ cm}^{-1}$  [28], respectively, to the  $\text{SiO}_2$  network band at around  $800\text{ cm}^{-1}$  and to the SiOH band at  $980\text{ cm}^{-1}$ . The R band of silica nanoparticles does not overlap any of the silicone or epoxy peaks and it could be exploited for nanoparticles identification in a mixture. A nanocomposite sample consisting of epoxy matrix and 5 vol.% homogeneously distributed silica nanoparticles was also measured. The obtained spectra only contain peaks of epoxy (data not shown). Signals from the amorphous silica nanoparticles embedded in the epoxy obviously are too weak to detect.

Fig.5 site 1 shows a typical spectrum of a carbon fibre. It shows only two major peaks, the D band at approximately  $1350\text{ cm}^{-1}$  for disordered carbon, and the G band at  $1580\text{ cm}^{-1}$  for graphitized carbon, in accordance with results from literature [29].

### **3.2 Impact of cleaning procedure on removal of silicone oil from the disc surface**

Comparison of Fig.2 with Fig.1a reveals that the intensity of silicone Raman signals are reduced significantly as a consequence of the cleaning procedures, although they do not disappear completely. One may still detect silicone oil on the steel disc after acetone cleaning in ultrasonic bath as demonstrated in Fig.2a where typical Raman bands appear in the spectrum range at  $3000\text{-}2800\text{ cm}^{-1}$ ,  $1600\text{-}1300\text{ cm}^{-1}$  and  $1200\text{-}1000\text{ cm}^{-1}$ . The disk was further ground with abrasive paper, which reduces or removes the silicone oil from the surface, as observed by a decreased intensity or a complete disappearance of silicone oil fingerprint in different positions of the disk (Fig.2b, c). Fig.2 b shows additional signals besides the silicone fingerprint which can be attributed to G, D and 2D bands of more or less disordered graphite. Since the latter bands were unobserved before, grinding must have transferred this carbonaceous material to the disc. Interestingly, Raman spectra taken from unused abrasive paper only revealed signals of SiC and a polymeric material similar to the epoxy shown in section 3.1. Only after having been used for grinding, G- and D-bands appear also in the spectra of the abrasive paper. This finding suggests that either a certain amount of the polymeric binder phase of the abrasive paper or the silicone residues at the disc surface have been degraded during grinding leading to the release of carbonaceous particles. Furthermore, some diffuse peaks appear in the range  $600\text{-}200\text{ cm}^{-1}$ , which may originate from iron oxides, as will be discussed later (see 3.3 and 3.4).

It should be mentioned that the intensity of the main silicone fingerprint is not uniformly distributed over the whole disc surface. Raman mapping can depict this. Fig.3 shows two examples of optical micrographs and their respective Raman maps produced by using

intensities obtained from windows around the major peak at  $2900\text{ cm}^{-1}$ . Partly, the sites of higher silicone intensity correspond to features of the optical micrograph (e.g. groove-like features or roughness troughs, but this is not always the case. The dark blue areas of the Raman maps, visible in the web version of the article (major part of the maps, except bright spots with dark cores in the printed version) correspond to Raman spectra like the one shown in Fig.2c. Here definitely all silicone oil residues have been removed.

### **3.3 Potential of RS for wear scar characterization**

Since in the previous sections the authors proved that RS is very sensitive in detecting silicone species, they were keen on to find the fingerprint after tribological testing. For such a study, they further investigated some of the wear scars, produced during rubbing hybrid nanocomposites against acetone-cleaned steel discs [3] by RS. Especially the test parameter  $p_v=3\text{ MPa}$   $1\text{ m/s}$  was selected for this study, because under these conditions the hybrid composites showed exceptional wear and friction properties compared to conventional composites (without nanofiller). As revealed in Fig.4a, the spectrum taken at the boundary of the wear track corresponds to the one shown in Fig.2a for the acetone-cleaned disc. The intensities of the peaks depend on the sites selected for measurement, as discussed in section 3.2. D and G bands of amorphous and graphitic carbon appear in the range  $1600\text{-}1300\text{ cm}^{-1}$  (Fig.4a), and they become dominant approaching the wear scar area (Fig.4b). Interestingly, the characteristic silicone peaks are missing completely in the spectrum taken in the wear scar whereas characteristic D and G peaks of carbon, indicating amorphous and graphite-like carbon, respectively, increase their intensity.

Furthermore, the additional sharp peaks occurring between  $200\text{ and }650\text{ cm}^{-1}$  could be attributed to iron oxides. Similar RS-results were obtained previously after ball milling of magnetite-graphite blends [30], and at the surface of brake discs [31]. The higher G/D peak intensity ratio of the present study compared to the previous ones may be attributed to the

presence of graphite nanoparticles revealed by high resolution imaging of stacks of graphene planes in the tribofilms produced by the hybrid nanocomposites, which also contained 8 vol.% of well-crystallized graphite [4].

In addition to the carbon fibres and graphite filler there are other sources of carbon, namely the epoxy matrix and silicone oil residues, which may be activated due to high flash temperatures reached during tribological tests at high pv-values. The evolution of G- and D-bands during a RS measurement with increased laser power (data not shown) confirmed the susceptibility of the epoxy material to thermal degradation. Furthermore, Raman spectra were acquired from the tribologically stressed face of a pin made from a hybrid composite consisting of 10 vol.% carbon fibres and 2 vol.% silica nanoparticles embedded in epoxy resin. As shown in Fig.5, different types of spectra developed depending on the position of the laser beam. As already discussed in 3.1, the typical spectrum of carbon fibres was acquired at position 1 indicating that the bright constituent seen in the optical micrograph corresponds to carbon fibres. Obviously, the spectra from carbon fibres and wear scar are identical, indicating amorphous carbon or highly disordered graphite. At position 2 the epoxy fingerprint was observed, whereas the darker area corresponding to position 3 shows an overlap of signals from epoxy and amorphous carbon. Since no carbon fibre is seen at this location a transformation of epoxy to carbonaceous material as a consequence of tribological stressing may have occurred. This possibility should be kept in mind, but needs further studies which are going beyond the scope of the present work. Another possible explanation for the appearance of D and G bands at tribologically stressed surfaces could be that tiny wear particles from carbon fibres were spread over the pin surface and also transferred to the disc. The latter was also confirmed by RS spectra taken from the wear scar at the disc surface after tribological testing with this specific pin. Since, contrary to the results shown in Fig.4, this pin did not contain graphite filler, graphite transfer cannot solely explain the carbon at the disc surface. Kasem et al. [32] also observed the production of carbon wear particles from carbon

fibres as well as particle flow between first bodies and formation of a carbon-based tribolayer for a carbon fibre reinforced carbon composite (C/C composite) [32]. In conclusion, we can state that a transfer of neither epoxy nor silicone to the disc surface but more or less of disordered graphite took place.

### **3.4 Supplementary SEM/EDS and TEM/EDS results**

An additional task was to remove silicone oil from the disc surface with a strong chemical solvent, namely toluene in addition to acetone. These efforts took place before application of RS for the identification of silicone residues. The result was checked by SEM/EDS which was very time-consuming and not very sensitive. Nevertheless, the outcome was that also with toluene cleaning, silicone residues were not to remove completely, and therefore these efforts were replaced by the grinding method. Fig.6 shows characteristic EDS spectra of a toluene-cleaned disc. Although more than 90 % of the spectra correspond to a) which reveals the expected steel composition (Fig.6a), we detected some few contaminated spots containing increased Si and Al content were detected as well. Increased Si-content without Al, as shown in Fig.6b, most likely corresponds to silicone oil residue, whereas the presence of both elements, Al and Si, corresponds to abrasive particles, i.e. residues from the grinding process. The latter were studied more comprehensively by TEM/EDS, but will not be presented here. In the following, we present TEM/EDS results obtained by FIB target preparation at wear scars of previously cleaned discs. This is for demonstrating the difficulties, which may arise with tribofilm characterization by this method if silicone residue was not to removed completely. Two types of wear scars were selected for this purpose. The first one, termed C, was produced during a pin-on-disc test with a conventional composite rubbing against a steel disc. This composite contained only 10 vol.% carbon fibres and 8 vol.% graphite. In order to preserve the tribofilm, pv was limited to 1 MPa·1 m/s because otherwise the wear rate would have increased drastically [3]. On the other hand, wear scar H was produced by testing a

hybrid composite, which contained 5 vol.% silica nanoparticles in addition to the carbon fibres and graphite, at  $p_v=3$  MPa 1m/s. Thus, the tribofilm corresponding to wear scar C should not contain Si, in contrast to the one of wear scar H for which a transfer of silica nanoparticles from the composite to the disc surface could occur. At least two TEM-specimens (FIB-lamella) were prepared from each wear scar in order to reveal site-specific differences.

Figures 7a, 7b, 8 and 9 show the results of the X-TEM investigations for wear scars C and H, respectively. All films are more or less structureless i.e. amorphous, at least at the shown magnification. In high resolution TEM some tiny nanocrystals of iron oxide and graphite were observed previously [4], but not shown here. The EDS-results show significant differences not only between wear scars C and H, but also between different sites within the same wear scar. The film shown in Fig.7a consists mainly of carbon with minor amounts of iron and oxygen. It is likely that this corresponds to a film of transferred epoxy, which might develop because of the low  $p_v$ -value, or a carbonaceous product formed from epoxy mixed with iron oxide. The latter may form by tribooxidation of the disc surface. In contrast to site 1, the film observed at site 2 (Fig.7b) contains a considerable amount of Si and an increased amount of oxygen, while carbon is reduced compared to site 1. Since Si is not contained in the composite and only to a very small amount in the steel, we are quite sure that the high Silicon-concentration indicated in Fig.7b is due to silicone oil residue, locally identified on the disc surfaces despite of the cleaning procedures, as shown in section 3.2. A further feature apparent in Fig.7b is that the same high amount of Si revealed in the film is also detected in the adjacent steel substrate and platinum cap layer. This observation suggests a contamination of the TEM-specimen surface by a Si-containing species. A possible scenario for producing this feature could be that some silicone oil residue trapped in surface grooves evaporates during final FIB milling and re-deposits at the lamella surface. Thus, contamination of the TEM-specimens during preparation may explain the problems occurring occasionally during

the TEM/EDS investigation. Fig.8 shows the cross-section of a tribofilm corresponding to wear scar H formed at high pv conditions on a re-ground disc, thus providing the lowest level of silicone contamination, as proved in section 3.2. Here the appearance of the film corresponds to our expectations. The elemental profiles clearly reproduce the transitions from substrate to film and from film to the platinum cap layer. Film composition is homogeneous and consists mainly of Si and O with minor amounts of Fe and C. These results are consistent with RS suggesting the presence of carbonaceous material and iron oxide (see [3]).

Furthermore, they indicate the presence of silica as the major constituent, which was not visible in RS because of the low sensitivity of RS towards S-O bonds.

Finally, Fig.9 shows the results of a cross-sectional TEM investigation at the surface of an acetone-cleaned disc prior to tribological testing. A silicone film is clearly visible in bright contrast filling groves and open surface cracks of the roughness profile of the steel disc. The EDS spectrum of area 01 reveals high oxygen, silicon and carbon, as well as low iron concentrations. Thus, elemental composition and element concentrations are similar as for the tribofilm observed for wear scar H (Fig.8). Only the carbon concentration approximately doubles for the silicone film compared to the silica-based tribofilm. The high carbon and chromium concentrations measured within the boxes 02 and 03, located in the steel substrate, are due to the spherical carbide (typical constituent of steel 100Cr6) visible in the centre of the TEM micrograph.

Despite of the similarity of composition the structure of the two films shown in Fig.8 and 9 are completely different. Whereas the silicone film is an organic material, the silica-based tribofilm is of inorganic nature. This results in completely different tribological behaviours for conventional and hybrid composites, as will be shown later. In particular, the absence of the silicone fingerprint in Raman spectra taken from wear scars suggest, that silicone oil will degrade during tribological stressing. On the other hand, the stable silica-based films were only observed for wear scars produced by hybrid composites containing silica nanoparticles at



high pv-values ( $> 1 \text{ MPa} \cdot \text{m/s}$ ). The excellent friction and wear performance observed under these conditions bases upon the formation of this type of tribofilm [3, 4].

### **3.5 Impact of cleaning procedure on tribological behaviour**

With the following series of pin-on-disc tests, we intended to find out whether different levels of silicon oil contamination exert an impact on the COF evolution. In order to make the system as simple as possible, 100Cr6 pins were rubbed against 100Cr6 discs either with the as received surface state (treated with silicone oil), after cleaning with acetone and after re-grinding of the sliding surface. The results are shown in Fig.10. Obviously, the degree of silicone oil contamination does not affect the finally attained COF. Only at the very beginning of the test there seems to be some boundary lubrication providing low friction during the first couple of minutes. Then the COF increases at first quickly and later on more slowly until it reaches its final steady state value at approximately 0.8 which is typical for a steel-on-steel contact [19, 20, 23]. These results corroborate previous findings leading to the conclusion that removal of a surface layer by grinding did not affect tribological test results if compared to acetone-cleaned 100Cr6 discs [4]. It is interesting to compare the latter results with the present ones, and therefore Fig.10 has been reproduced from [4]. Apparently, no difference of COF evolution reveals while applying acetone-cleaned or additionally ground discs for the two composites tested here.

On the other hand, at the given stressing conditions ( $p_v=3 \text{ MPa} \cdot \text{m/s}$ ), friction and wear (the latter not shown here, but in [3]) of the two composites tested against steel discs is completely different. The beneficial tribofilm leading to the lower curve in Fig.11 corresponds to the one shown in Fig.8. This clearly demonstrates the advantage of the hybrid composite (H) compared to the conventional one (C). If the conventional composite is tested under the same conditions wear rates increase significantly and the originally formed carbonaceous tribofilm is destroyed. Simultaneously the COF increases up to a final value of 0.8, very similar to that

of the steel-on-steel contact shown in Fig.10. Although this value is compatible with values known for steel-on-steel contacts, it also may be attributed to the presence of iron oxide between the first bodies of the friction couple. COF-values between 0.55 and 0.8 were measured by pin-on-disc tests during the supply of various  $\text{Fe}_2\text{O}_3$ -powders [4, 20], depending on the grain size of the powder particles.

#### **4. Final discussion and outlook**

Although it has become clear that silicone oil cannot be removed completely from steel disc surfaces, it has been shown that this will not affect long-term tribological properties. This is because the silicone is not stable under most tribological conditions and thus will either leave the contact area as a gas or stay there as carbonaceous particles. Since there are a number of different sources of carbonaceous particles if polymer matrix composites are rubbing against steel discs, the presence or absence of silicone will not make much difference.

The main objective of the present, previous and future studies is to determine the structure of beneficial tribofilms and find explanations for their good anti-friction and anti-wear properties. There is no doubt that silica nanoparticles not only increase the strength of epoxy-based composites, but that they also are responsible for low friction and wear rates at high pv-values when conventional composites fail. A simple transfer of SNPs from a hybrid composite to the steel disc forming a glassy layer of silica can explain wear reduction, but not the observed COF decrease. Actually, pin-on-disc tests with the supply of silica nanoparticles provided a high COF of at least 0.7 [4] instead of 0.1 observed for the hybrid composite (H) in Fig.11. The application of RS, but also of other techniques (Fig.8 and [4]) shows that the beneficial tribofilm does not only contain amorphous silica, but also  $\text{Fe}_2\text{O}_3$  and carbonaceous material. In some cases Österle et al. observed graphite-like species by TEM [4]. Furthermore, mixing the silica with iron oxide did not change the friction behaviour, whereas mixing it with graphite reduced the COF significantly. Since EDS-results are not very reliable in terms of C-

quantification, it is difficult to prove the presence of carbonaceous species in the tribofilms by this method. On the other hand, RS is very sensitive for revealing carbonaceous species and distinguishing between silicone and epoxy, whereas silica signals are very weak. Thus, a combination of both methods is beneficial. Since neither epoxy nor silicone were revealed in wear scars by RS, we conclude that both species were degraded during tribological stressing and either removed from the contact by evaporation or incorporated into the forming tribofilm as carbonaceous particles. Thermal degradation of the epoxy matrix can also explain the release of silica nanoparticles from the hybrid composite and formation of a silica-based tribofilm at the disc surface. The low COF of the tribofilm may be due to embedding of either wear particles from carbon fibres, graphite filler or degradation products from epoxy and silicone into the silica film. Different authors [32, 33] showed the evolution of nanometer-sized particles from carbon fibre reinforced carbon materials. The formation of these particles has been correlated with a smooth sliding behaviour at a relatively high friction level (COF=0.4). The low COF of 0.1 observed for the hybrid composite at high pv-values may be due to transformation of amorphous carbon to graphite nanoparticles, a soft constituent, which if mixed with silica nanoparticles provides low friction [4]. Evidence for such a transformation was obtained for an amorphous carbon coating which also showed exceptional low COF under dry sliding conditions [34]. Furthermore, hydrogenated amorphous carbon particles, which may form as degradation products of epoxy, are known to provide low friction as well [34]. A recent study based on molecular dynamics showed that even very hard tetragonal carbon, i.e. diamond or ta-C, is transformed to soft amorphous wear debris during tribological stressing [35]. We hope that a deeper understanding of the sliding behaviour of silica-based tribofilms with soft nanoinclusions will be obtained by applying nanoscopic modelling in the future. Previously, Österle et al. showed that a nanocomposite film consisting of a relatively hard and brittle oxide mixed with soft nanoparticles provides smooth

sliding at a significantly decreased COF compared to the pure oxide [36]. Similar modelling efforts are planned now for the silica-based tribofilm.

## **5. Conclusions**

Raman spectroscopy is very useful not only for detecting small amounts of silicone oil, but also for the localization of silicone oil residues at steel surfaces. It has been shown that after chemical cleaning with acetone and toluene, and even after the removal of a 100  $\mu\text{m}$  thick surface layer by grinding, silicone residues are still present at some surface sites.

For TEM-characterization of tribofilms, while applying the FIB technique for lamella preparation, it is essential to select silicone-free areas, because otherwise contamination of the TEM-specimens may occur leading to forged EDS results.

Since RS of wear scars revealed neither epoxy nor silicone oil fingerprints but only signals of carbonaceous material, this leads to the conclusion that both constituents were not stable during the applied tribological stressing but degraded to carbonaceous, hydrocarbon or siloxane-like species. Further characterization of such degradation products by IR spectroscopy will be done in the future.

Long-term tribological properties were not affected by the amount of silicone oil residues at the disc surface, but rather by the silica nanoparticles, which are contained in the hybrid composites but not in the conventional composites. Thus, we conclude that the silica-based tribofilm observed at the disc surface after testing at high  $p_v$ -values is responsible for the observed superior wear and friction behaviour.

## **Acknowledgements**

The German Research Foundation funded this work under contract numbers: OS 77/20-1 and ZH 352/3-1 and RFBR research project No. 14-08-91330 HHIO. A.I.D. also thanks the Tomsk State University Academic D.I. Mendeleev Fund Program in 2014- 2015. Finally the

authors would like to thank Arno Eberle for his valuable assistance during editing the English text.

## References

- [1] Rong MZ, Zhang MQ, Liu H, Zeng HM, Wetzel B, Friedrich K. Microstructure and tribological behavior of polymeric nanocomposites. *Ind Lubr Tribol* 2001; 53: 72-7.
- [2] Zhang G. Structure-tribological property relationship of nanoparticles and short carbon fibers reinforced PEEK hybrid composites. *J Polym Sci Part B: Polym Phys* 2010; 48: 801-11.
- [3] Zhang G, Sebastian R, Burkhart T, Friedrich K. Role of monodispersed nanoparticles on the tribological behavior of conventional epoxy composites filled with carbon fibers and graphite lubricants. *Wear* 2012; 292-293: 176-87.
- [4] Österle W, Dmitriev AI, Gradt T, Häusler I, Hammouri B, Morales Guzman PI, Wetzel B, Zhang G, Yigit D. Exploring the beneficial role of tribofilms formed from an epoxy-based hybrid nano-composite. *Tribol Int* 2015; 88: 126-34.
- [5] Zhang G, Wetzel B, Jim B, Österle W. Impact of counterface topography on the formation mechanisms of nanostructured tribofilm of PEEK hybrid nanocomposites. *Tribol Int* 2015; 83:156-65.
- [6] Sebastian R, Noll A, Zhang G, Burkhart T, Wetzel B. Friction and wear of PPS/CNT nanocomposites with formation of electrically isolating transfer films. *Tribol Int* 2013; 64: 187-95.
- [7] Friedrich K, Knoer N, Almajid AA. Processing-Structure-Property Relationships of Thermoplastic Nanocomposites used in Friction and Wear Applications. *Mechanics of Composite Materials* 2012; 48: 179-92.

- [8] Noll A, Friedrich K, Burkhart T, Breuer U. Effective multifunctionality of poly(p-phenylene sulfide) nanocomposites filled with different amounts of carbon nanotubes, graphite, and short carbon fibers. *Polymer Composites* 2013; 34: 1405-12.
- [9] Pei X, Friedrich K. Sliding wear properties of PEEK, PBI and PPP. *Wear* 2012; 274: 452-5.
- [10] Pei X, Evstatiev M, Friedrich K. Mechanical and Tribological Properties of PET/HDPE MFCs. *International Journal of Polymeric Materials* 2012; 61: 963-77.
- [11] Rasheva Z, Zhang G, Burkhart T. A correlation between the tribological and mechanical properties of short carbon fibers reinforced PEEK materials with different fiber orientations. *Tribol Int* 2010; 43: 1430-7.
- [12] Zhang G, Rasheva Z, Schlarb AK. Friction and wear variations of short carbon fiber (SCF)/PTFE/graphite (10 vol.%) filled PEEK: Effects of fiber orientation and nominal contact pressure. *Wear* 2010; 268: 893-9.
- [13] Gyurova LA, Friedrich K. Artificial neural networks for predicting sliding friction and wear properties of polyphenylene sulfide composites. *Tribol Int* 2011; 44: 603-9.
- [14] Chang L, Friedrich K. Enhancement effect of nanoparticles on the sliding wear of short fiber-reinforced polymer composites: A critical discussion of wear mechanisms. *Tribol Int* 2010; 43: 2355-64.
- [15] Friedrich K, Burkhart T, Almajid AA, Hauptert F. Poly-Para-Phenylene-Copolymer (PPP): A High-Strength Polymer with Interesting Mechanical and Tribological Properties. *International Journal of Polymeric Materials* 2010; 59: 680-92.
- [16] Zhang G, Chang L, Schlarb AK. The roles of nano-SiO<sub>2</sub> particles on the tribological behavior of short carbon fiber reinforced PEEK. *Composites Science and Technology* 2009; 69: 1029-35.
- [17] Theiler G, Hübner W, Gradt T, Klein P, Friedrich K. Friction and Wear of PTFE-Composites at Cryogenic Temperatures. *Tribol Int* 2002; 35: 449-58.

- [18] Theiler G, Gradt T. Influence of the Temperature on the Tribological Behaviour of PEEK Composites in Vacuum Environment. PROCEEDINGS OF THE 17TH INTERNATIONAL VACUUM CONGRESS/13TH INTERNATIONAL CONFERENCE ON SURFACE SCIENCE/INTERNATIONAL CONFERENCE ON NANOSCIENCE AND TECHNOLOGY: Book Series: Journal of Physics Conference Series, Johansson LSO, Andersen JN, Gothelid M; et al. (eds.) Volume: 100 Article Number: 072040 Published: 2008
- [19] Österle W, Deutsch C, Gradt T, Orts-Gil G, Schneider T, Dmitriev AI. Tribological screening tests for the selection of raw materials for automotive brake pad formulations. Tribol.Int. 2014; 73: 148-55.
- [20] Kato H. Severe-mild wear transition by supply of oxide particles on sliding surface. Wear 2003; 255: 426-9.
- [21] Lemm JD, Warmuth AR, Pearson SR, Shipway PH. The influence of surface hardness on the fretting wear of steel pairs – Its role in debris retention in the contact. Tribol Int 2015; 81: 258-66.
- [22] Popov V, Psakhie SG, Shilko EV, Dmitriev AI, Knothe K, Bucher F, Ertz M. Friction coefficient in rail-wheel contacts as a function of material and loading parameters. Physical Mesomechanics 2002; 5: 17-24.
- [23] Areiza YA, Garces SI, Santa JF, Vargas G, Toro A. Field measurement of coefficient of friction in rails using a hand-pushed tribometer. Tribol Int 2015; 82: 274-9.
- [24] Czichos H. Tribology – A System Approach to the Science and Technology of Friction, Lubrication and Wear. Elsevier, Amsterdam 1978.
- [25] Handbook of Vibrational Spectroscopy; Chalmers, J.M., Griffiths, P.R., Eds.; John Wiley & Sons Ltd., Chichester, UK, 2002.
- [26] Infrared and Raman Characteristic Group Frequencies. Tables and Charts. Socrates G. (ed.), John Wiley & Sons Ltd. England, 2001.

- [27] Vaskova H., Kresalek V., Raman spectroscopy of epoxy resin crosslinking. 11 Proceedings of the 13th WSEAS international conference on Automatic control, modelling & simulation. 2011; 357-61.
- [28] Galeener FL, Geissberger AE. Vibrational dynamics in Si<sub>30</sub>-substituted vitreous SiO<sub>2</sub>. Phys Rev B 1983; 27: 6199-204.
- [29] Roh JS. Structural study of the activated carbon fiber using Laser Raman Spectroscopy. Carbon Letters 2008; 9-2: 127-30.
- [30] Österle W, Orts-Gil G, Gross T, Deutsch C, Hinrichs R, Vasconcellos MAZ, Zoz H, Yigit D, Sun X. Impact of high energy ball milling on the nanostructure of magnetite-graphite and magnetite-graphite-molybdenum disulphide blends. Materials Characterization 2013; 86: 26-38.
- [31] Vasconcellos MAZ, Soares MRF, Hinrichs R. Layered structure of friction films revealed by the comparison between multi-energy x-ray microanalysis and Monte Carlo simulations. Wear 2012; 294-295: 347-55.
- [32] Kasem H, Bonnamy S, Berthier Y, Dufrenoy P, Jacquemard P. Tribological, physicochemical and thermal study of the abrupt friction transition during carbon/carbon composite friction. Wear 2009; 267: 846-52.
- [33] Lei B, He L, Yi M, Ran L, Xu H, Ge Y, Peng K.: New insights into the microstructure of the friction surface layer of C/C composites. Carbon 2011; 49: 4554-62.
- [34] Pei YT, Galvan D, De Hosson JTM, Cavaleiro A. Nanostructured TiC/a-C coatings for low friction and wear resistant applications. Surface & Coatings Technology 2005; 198: 44-50.
- [35] Kunze T, Posselt M, Gemming S, Seifert G, Konicek, R, Carpick RW, Pastewka L, Moseler M. Wear, plasticity, and rehybridization in tetragonal amorphous carbon. Tribol Lett 2014; 53: 119-26.



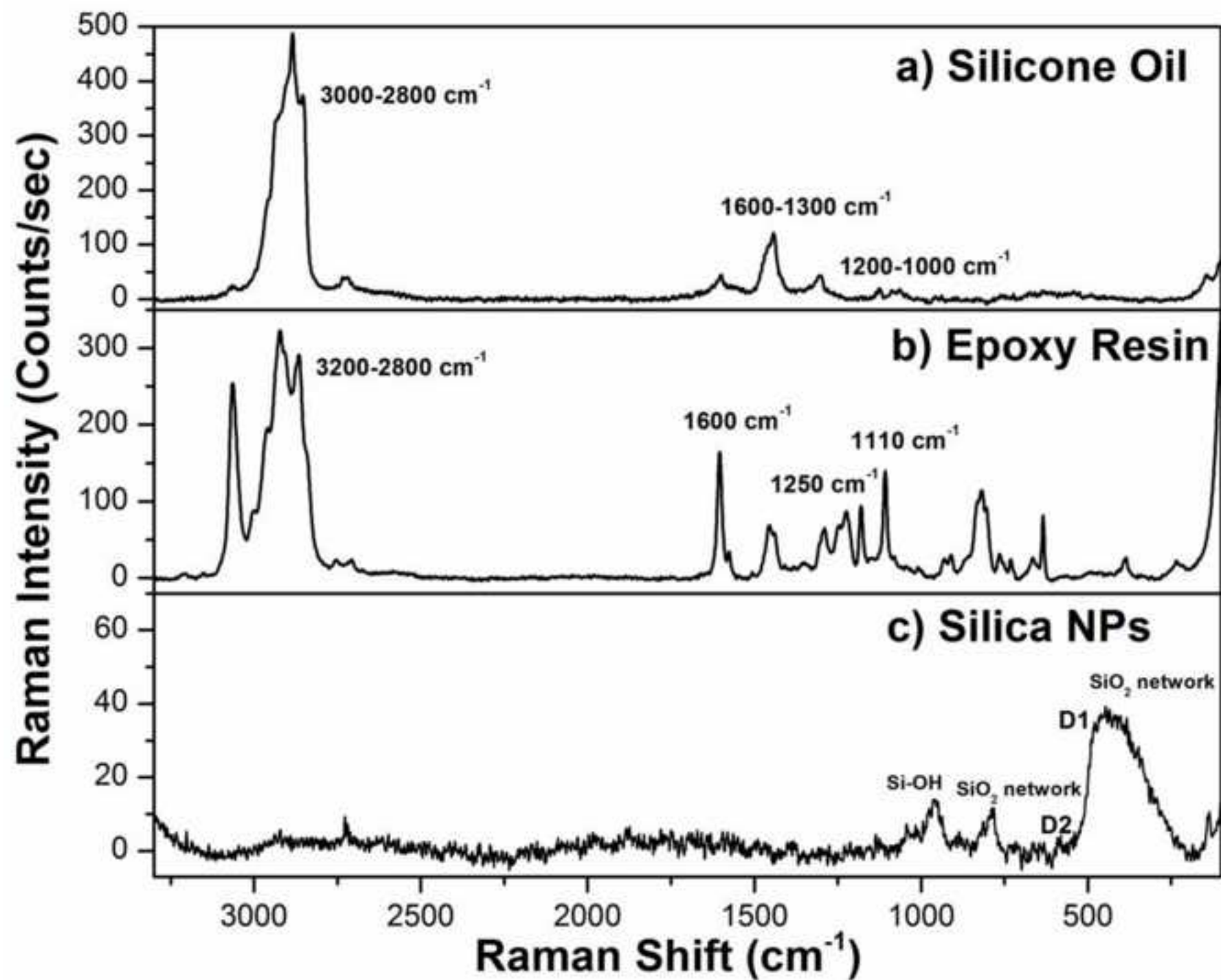
- [36] Österle W, Dmitriev AI, Orts-Gil G, Schneider T, Ren H, Sun X. Verification of nanometre-scale modelling of tribofilm sliding behaviour. *Tribol Int* 2013; 62: 155-62.

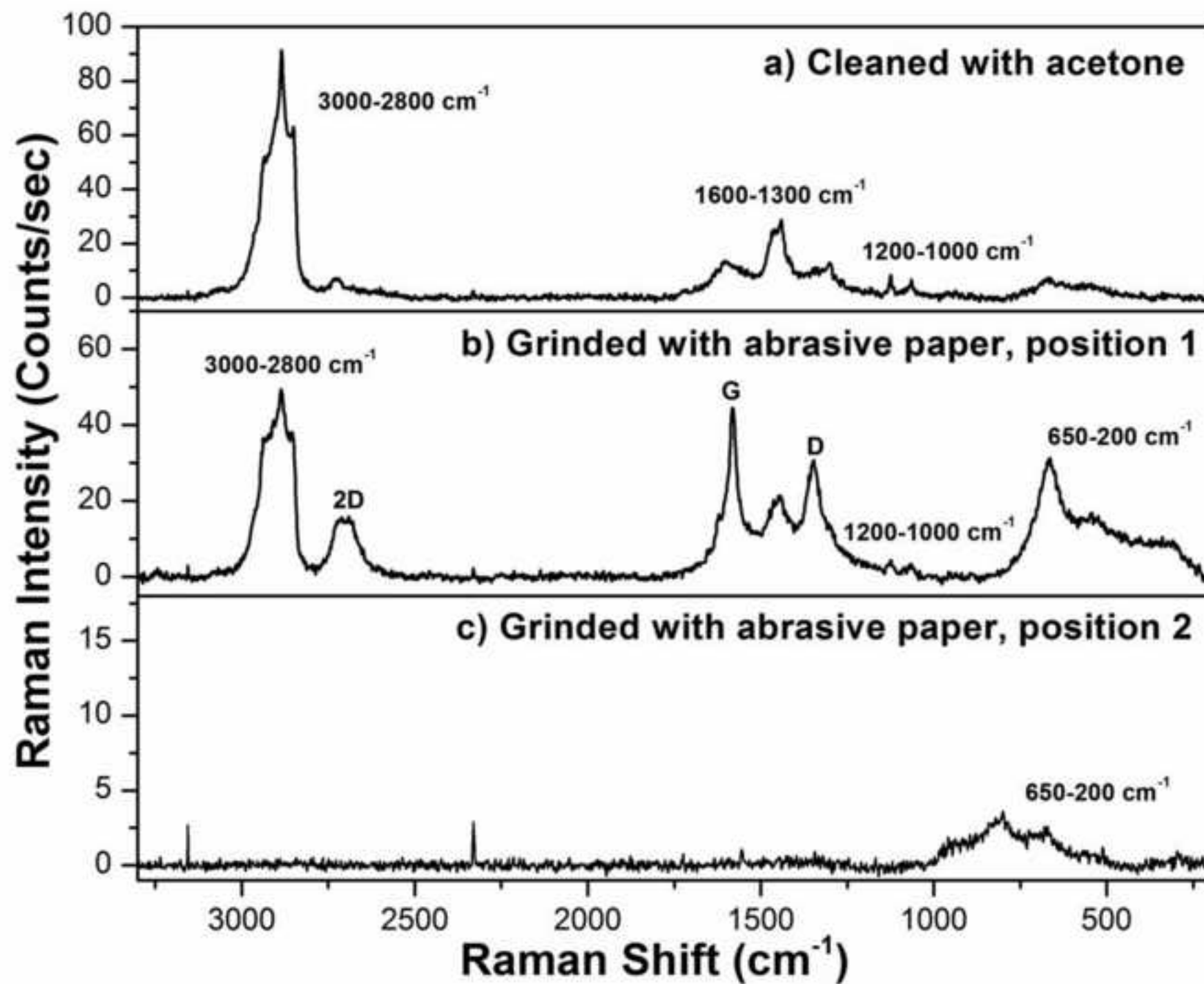
## Table Caption

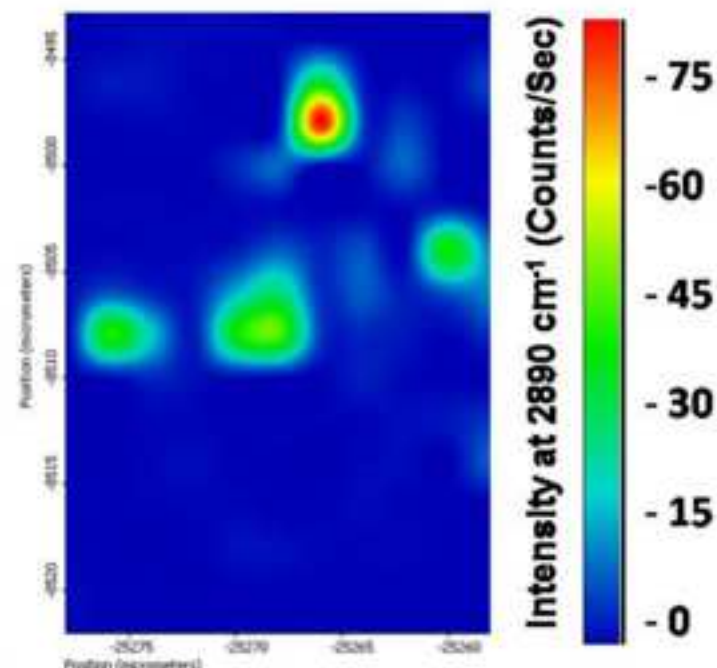
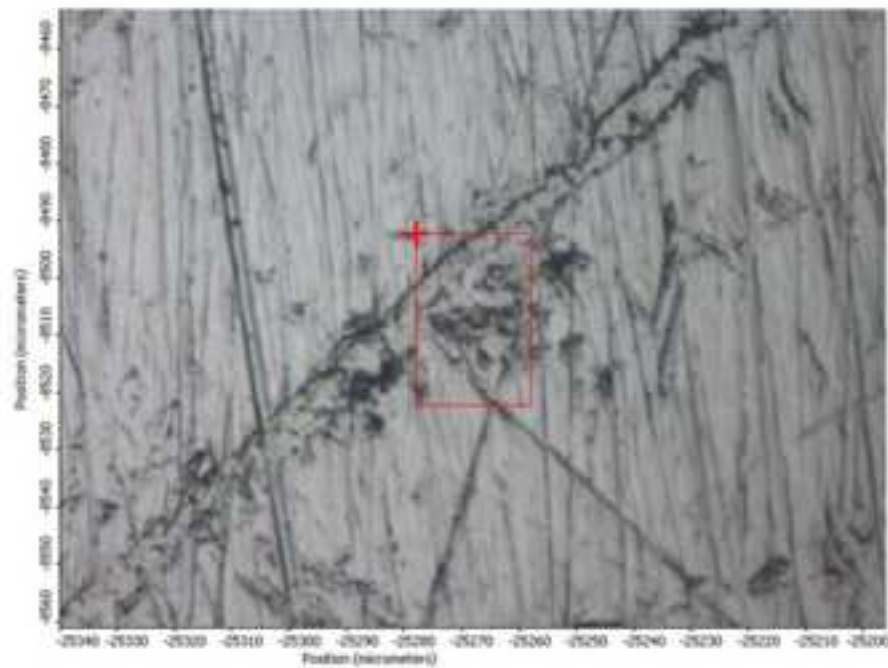
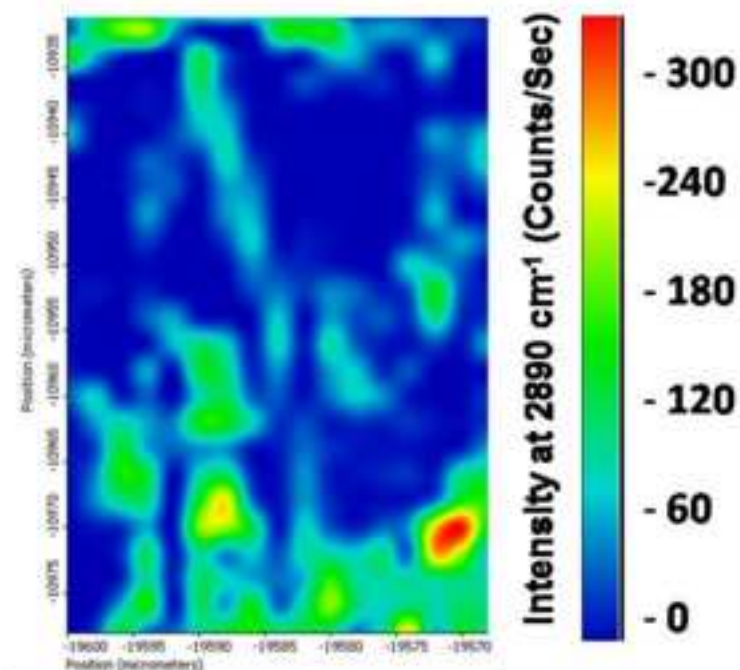
Table 1      Test matrix indicating testing conditions, surface states of 100Cr6 discs and corresponding characterization results

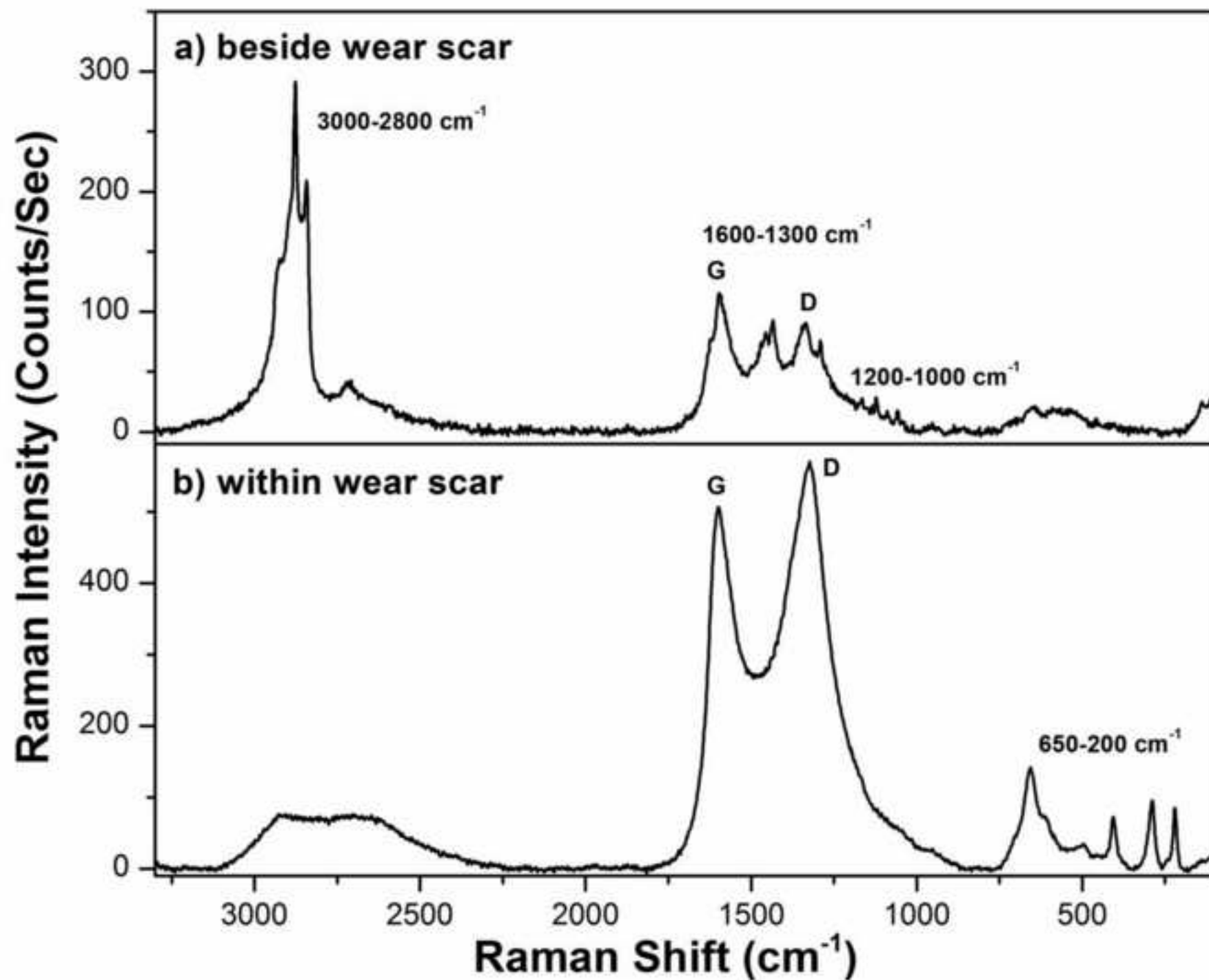
## Figure Captions

- Fig.1 Raman spectra of pure ingredients
- Fig.2 Impact of cleaning procedure on Raman spectra acquired at disc surfaces
- Fig.3 Optical micrographs and silicone Raman maps corresponding to marked boxes after different cleaning procedures:  
Acetone-cleaned (top), ground with abrasive paper (bottom).  
For interpretation of the references to color in this figure legend, the reader is referred to the web version of the article
- Fig.4 Comparison of RS within and outside of a wear scar of the steel disc
- Fig.5 Raman spectra acquired from the surface of a rubbed composite pin comprising of epoxy mixed with 10 vol.% carbon fibers and 2 vol.% silica nanoparticles
- Fig.6 EDS-results after chemical cleaning with toluene and acetone, a) blank steel surface, b) local silicone contamination at disc surface, c) abrasive particle at disc surface
- Fig.7 X-TEM micrographs and EDS-line scans at two different sites of wear scar C (conventional composite slid against acetone-cleaned 100Cr6 disc at  $p_v=1 \text{ MPa} \cdot 1 \text{ m/s}$ ), a) site 1, b) site 2.  
In b) the profile of O is always above the one of Pt, which is depicted clearly by color in the web version of the article.
- Fig.8 X-TEM micrograph and EDS line scan of wear scar H (hybrid composite slid against ground 100Cr6 disc at  $p_v=3 \text{ MPa} \cdot 1 \text{ m/s}$ )
- Fig.9 X-TEM micrograph and EDS spectra of acetone-cleaned 100Cr6 disc prior to testing. The spectrum corresponding to area 01 corroborates the presence of a silicone film at the disc surface.
- Fig.10 COF evolution during pin-on-disc tests, a) without cleaning (as received), b) after cleaning with acetone, c) after grinding with abrasive paper
- Fig.11 Impact of surface treatment on COF evolution at  $p_v=3 \text{ MPa} \cdot 1 \text{ m/s}$  for conventional composite (C) and hybrid composite (H) (reproduced from [4])

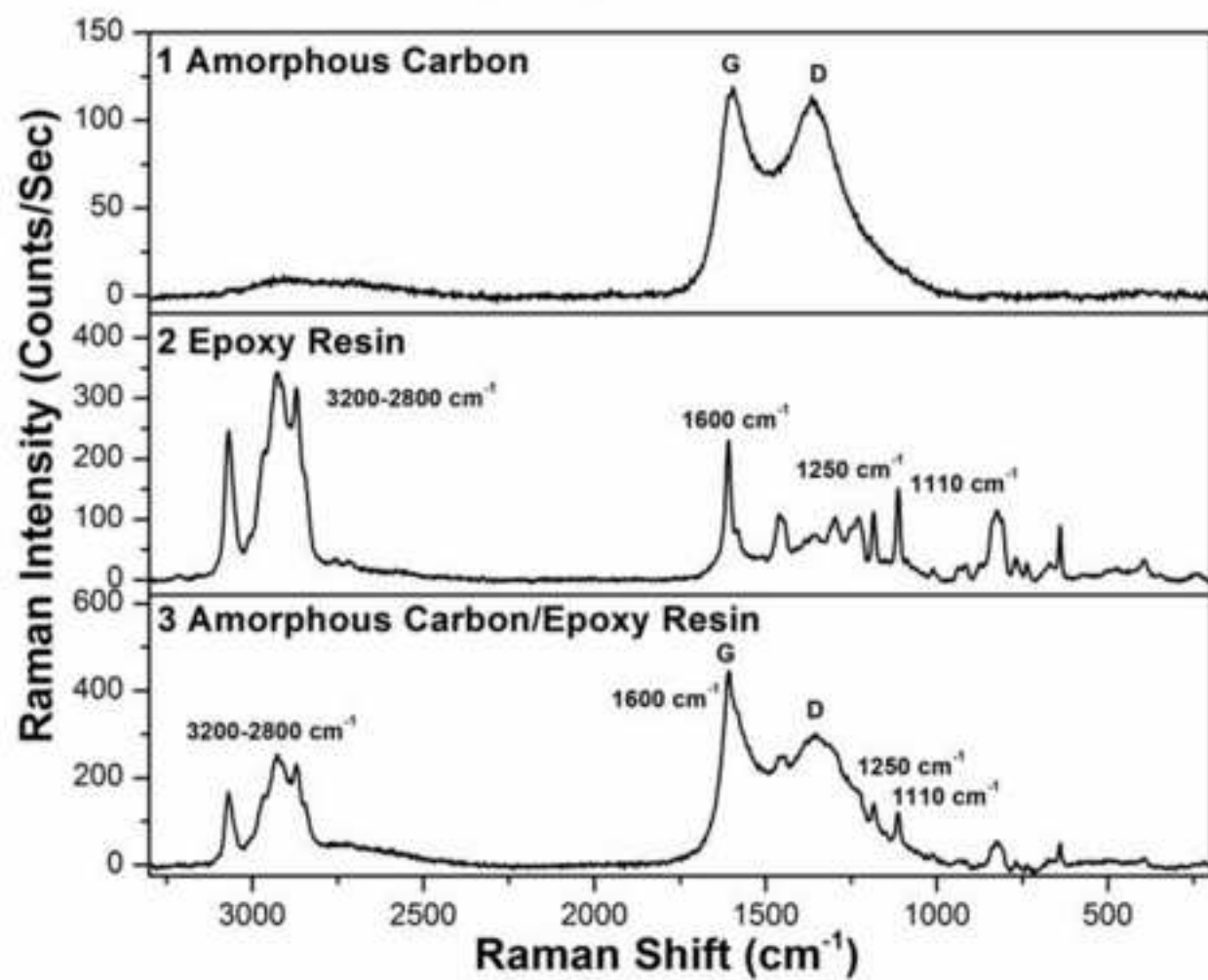


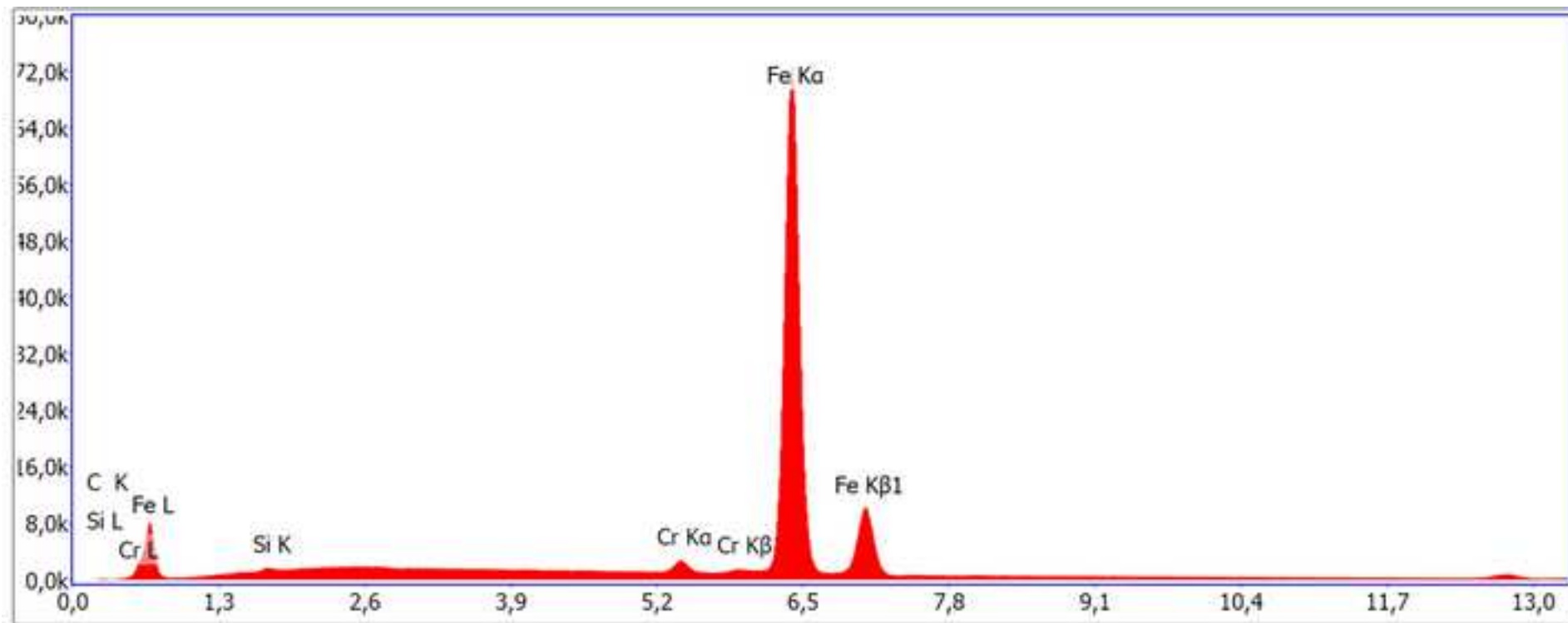






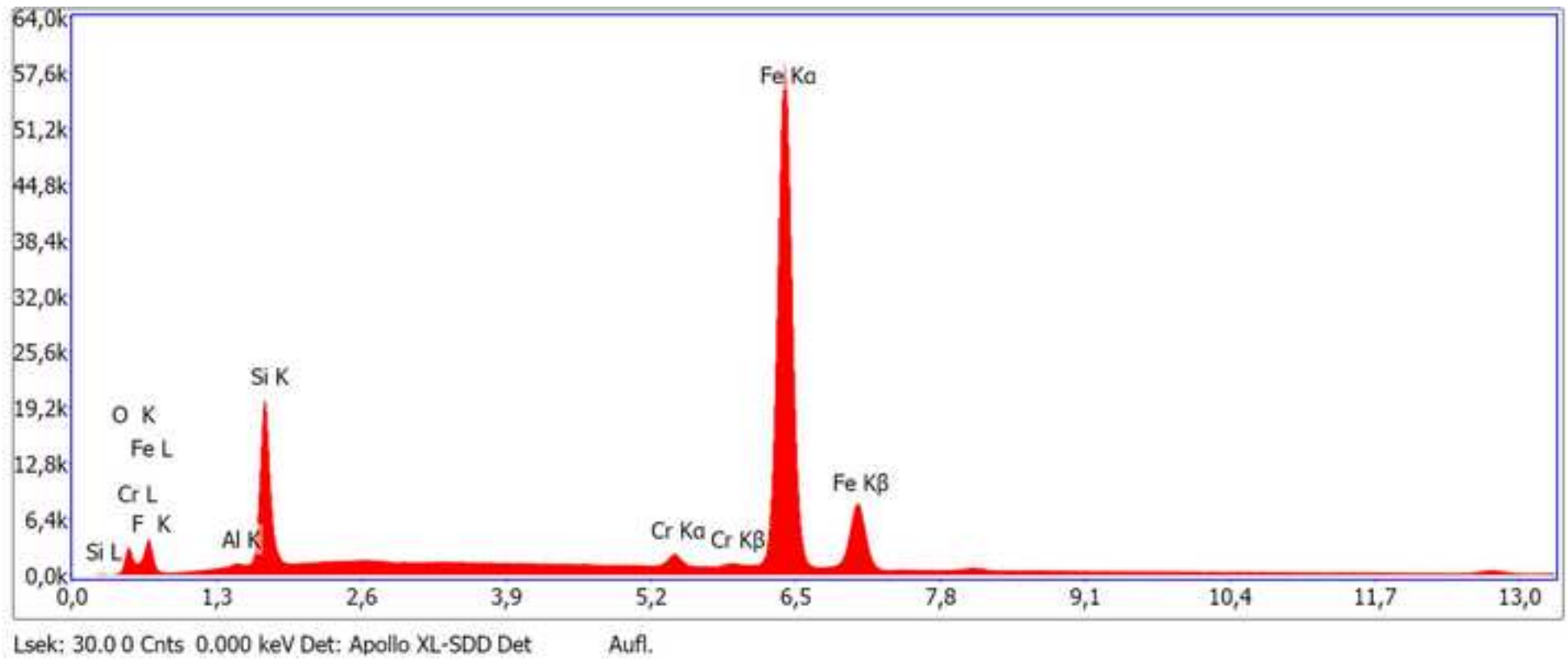




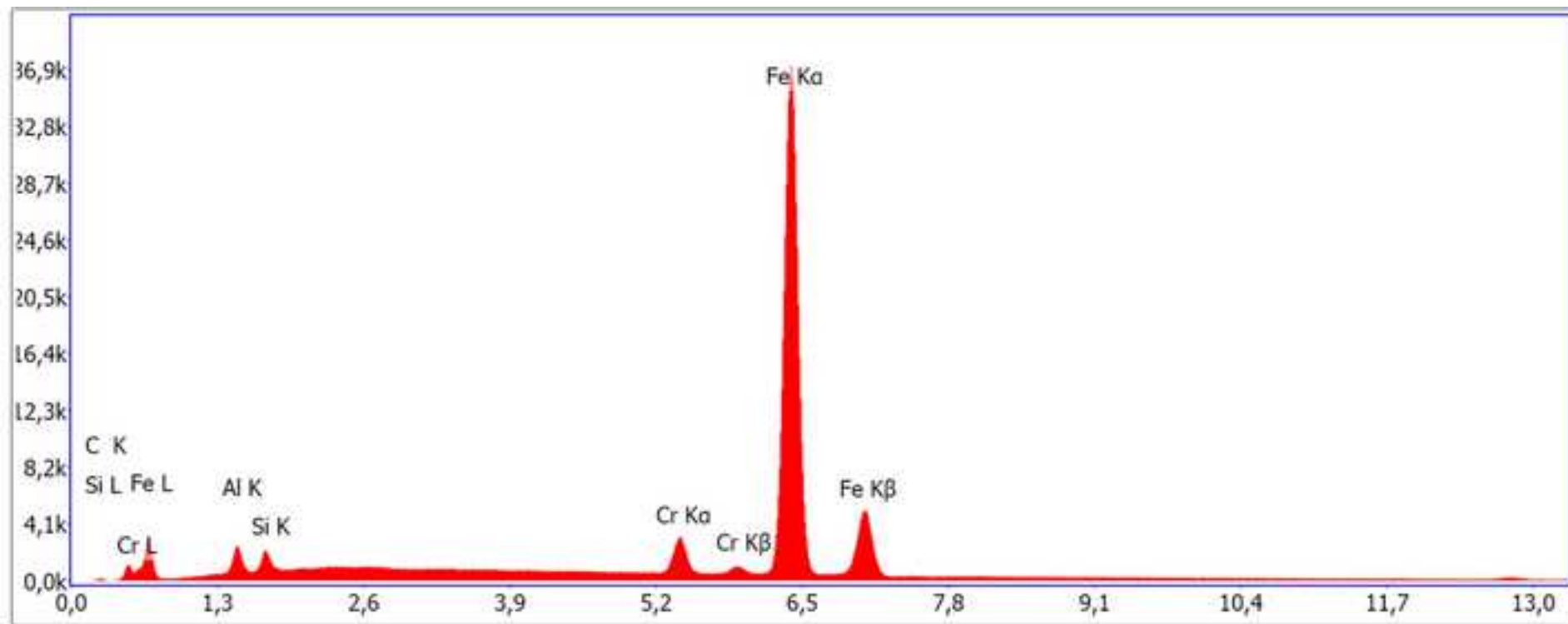


Lsek: 30.0 0 Cnts 0.000 keV Det: Apollo XL-SDD Det

Aufi.

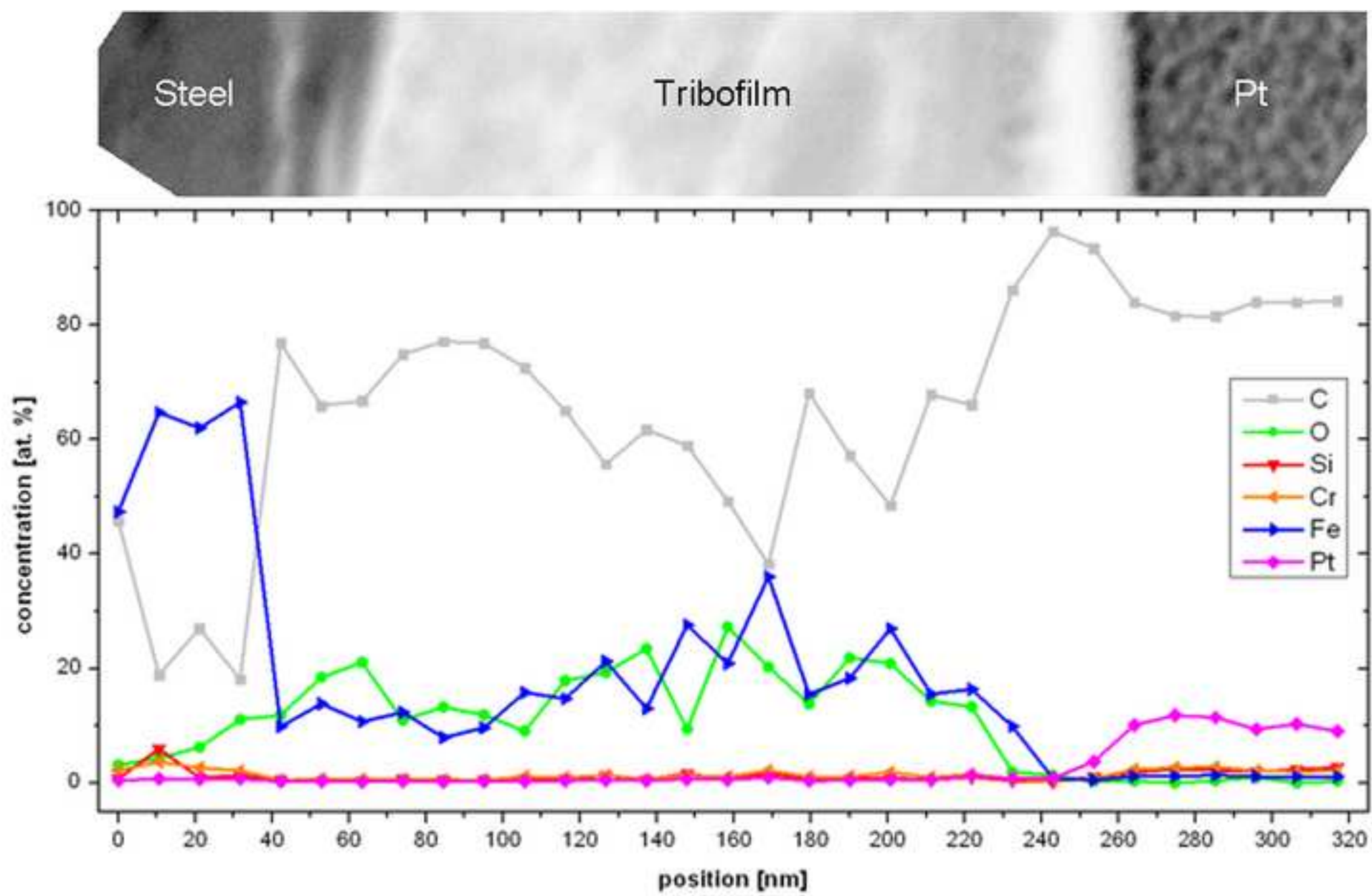






Lsek: 30.0 0 Cnts 0.000 keV Det: Apollo XL-SDD Det

Aufi.



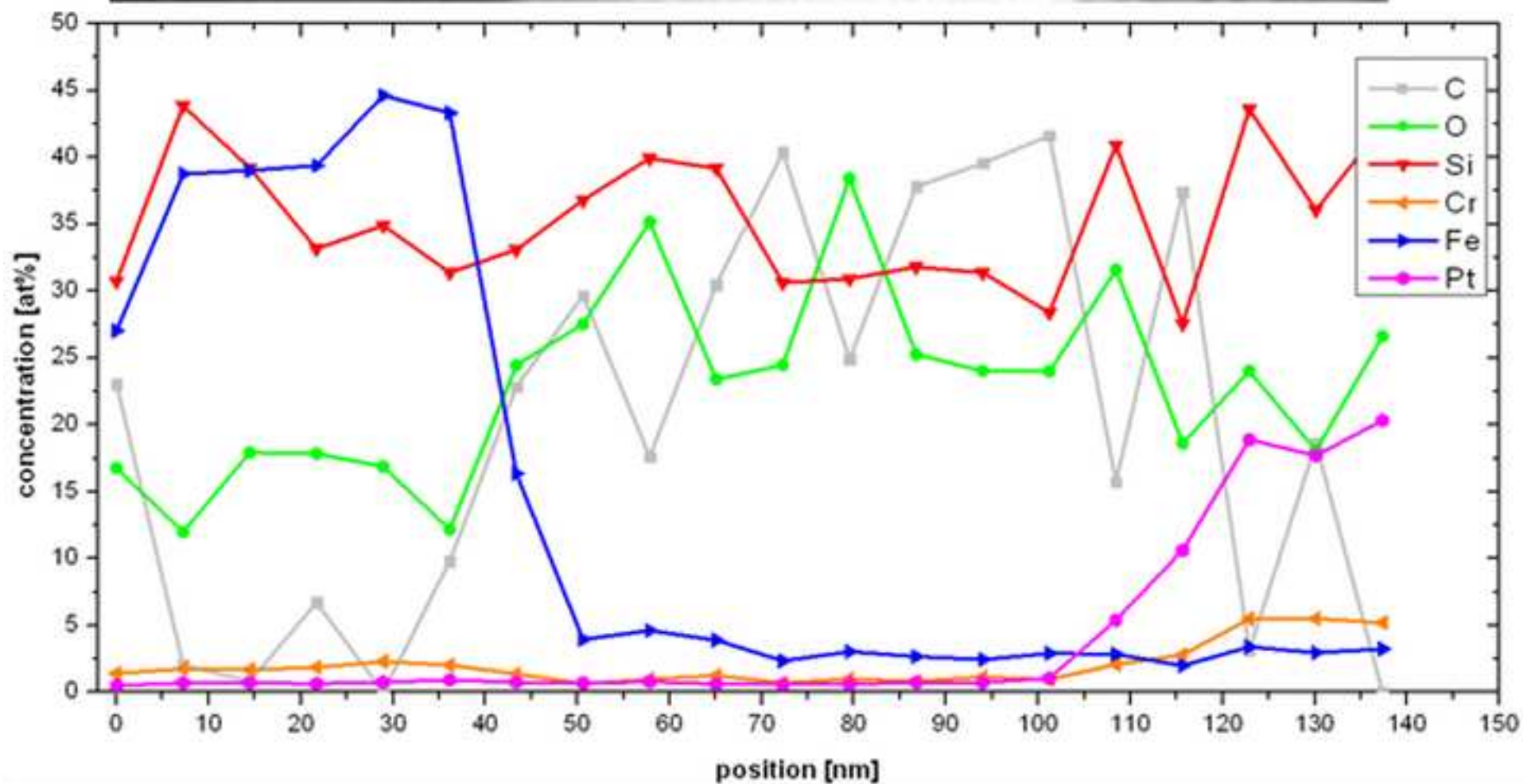


Fig8

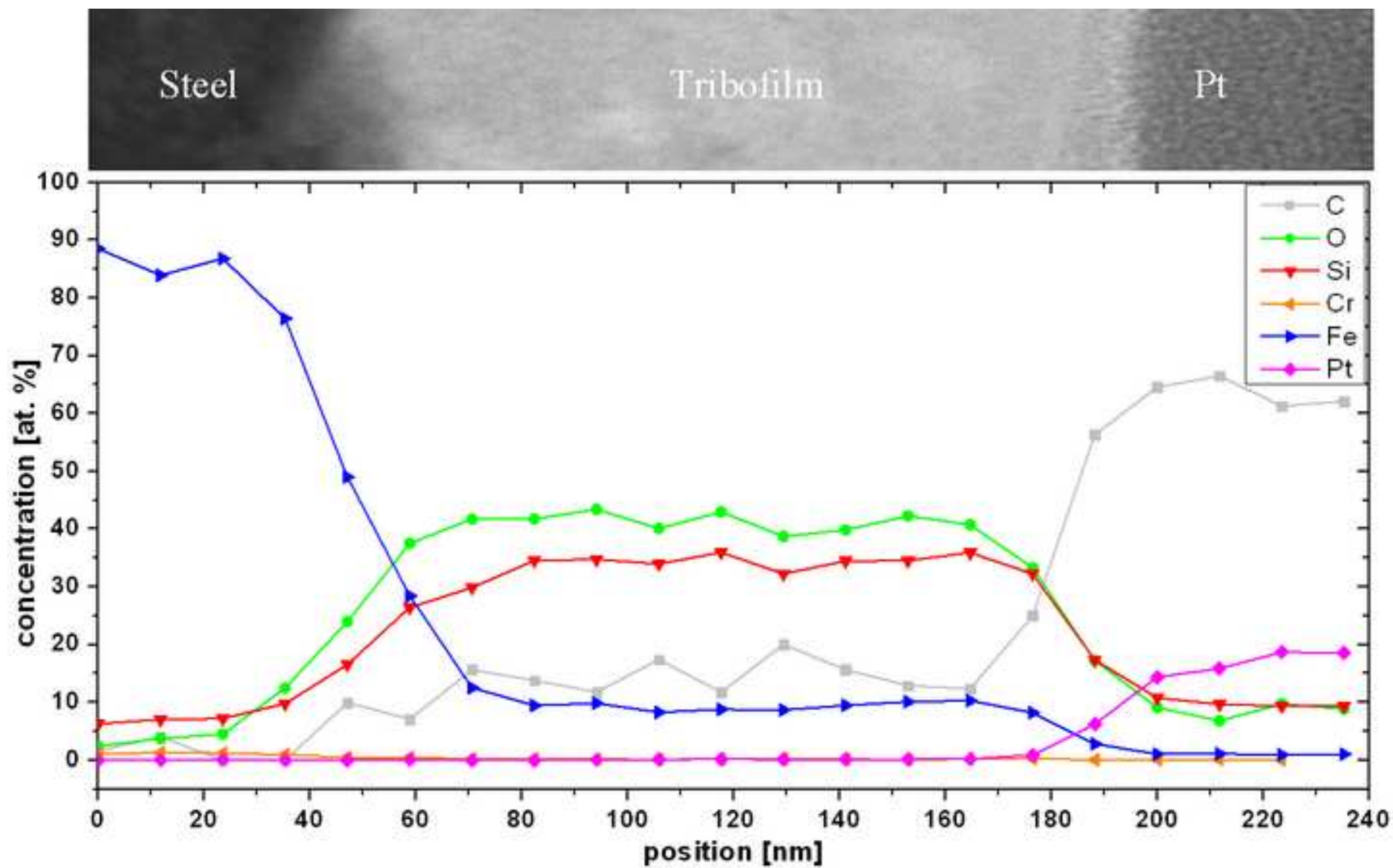


Fig9

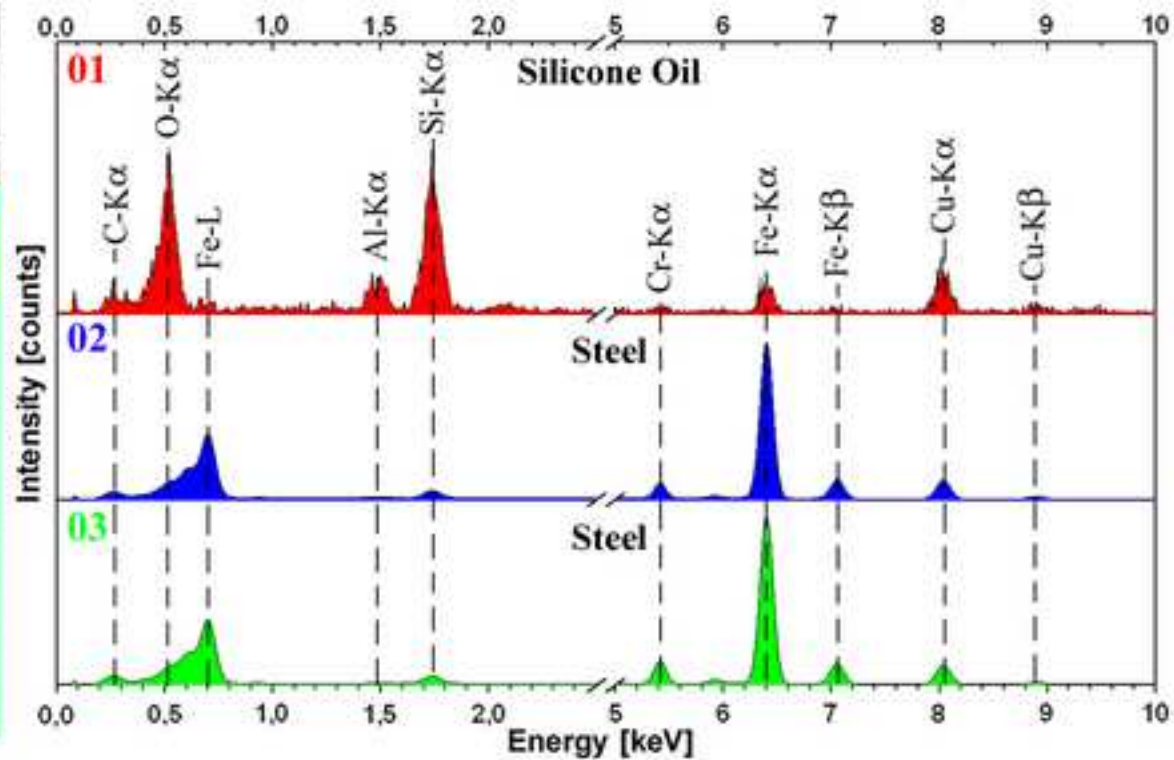
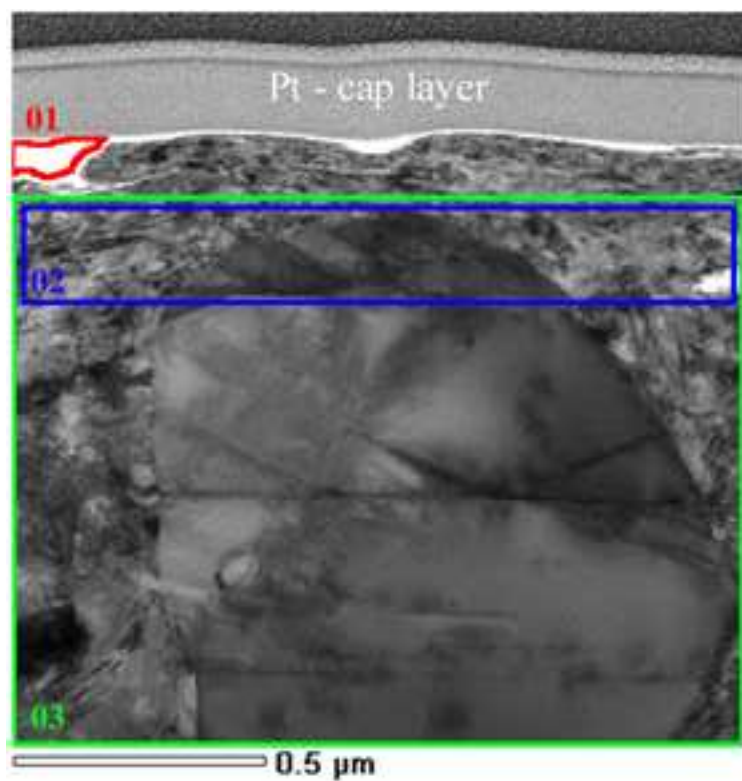




Fig10a

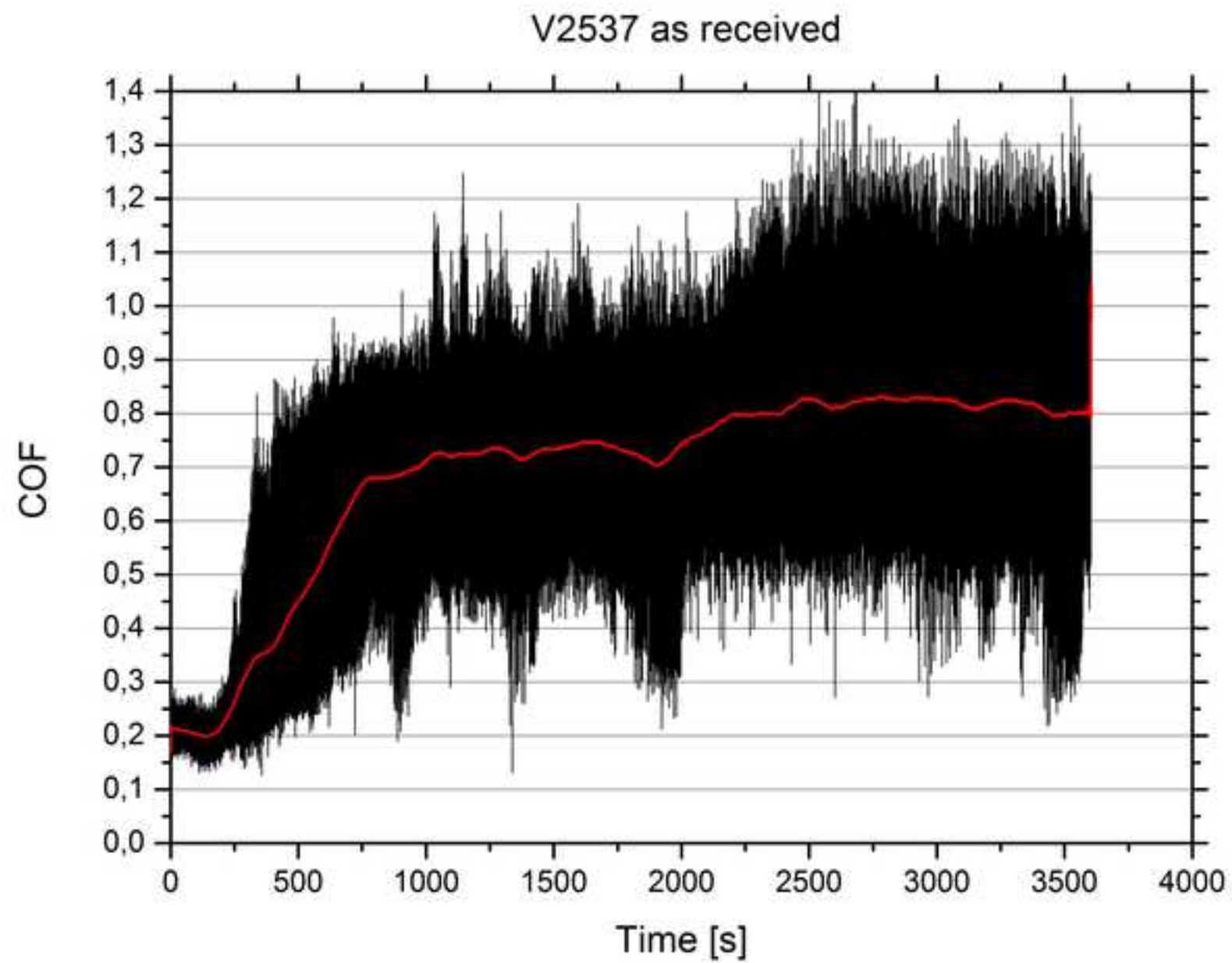


Fig10b

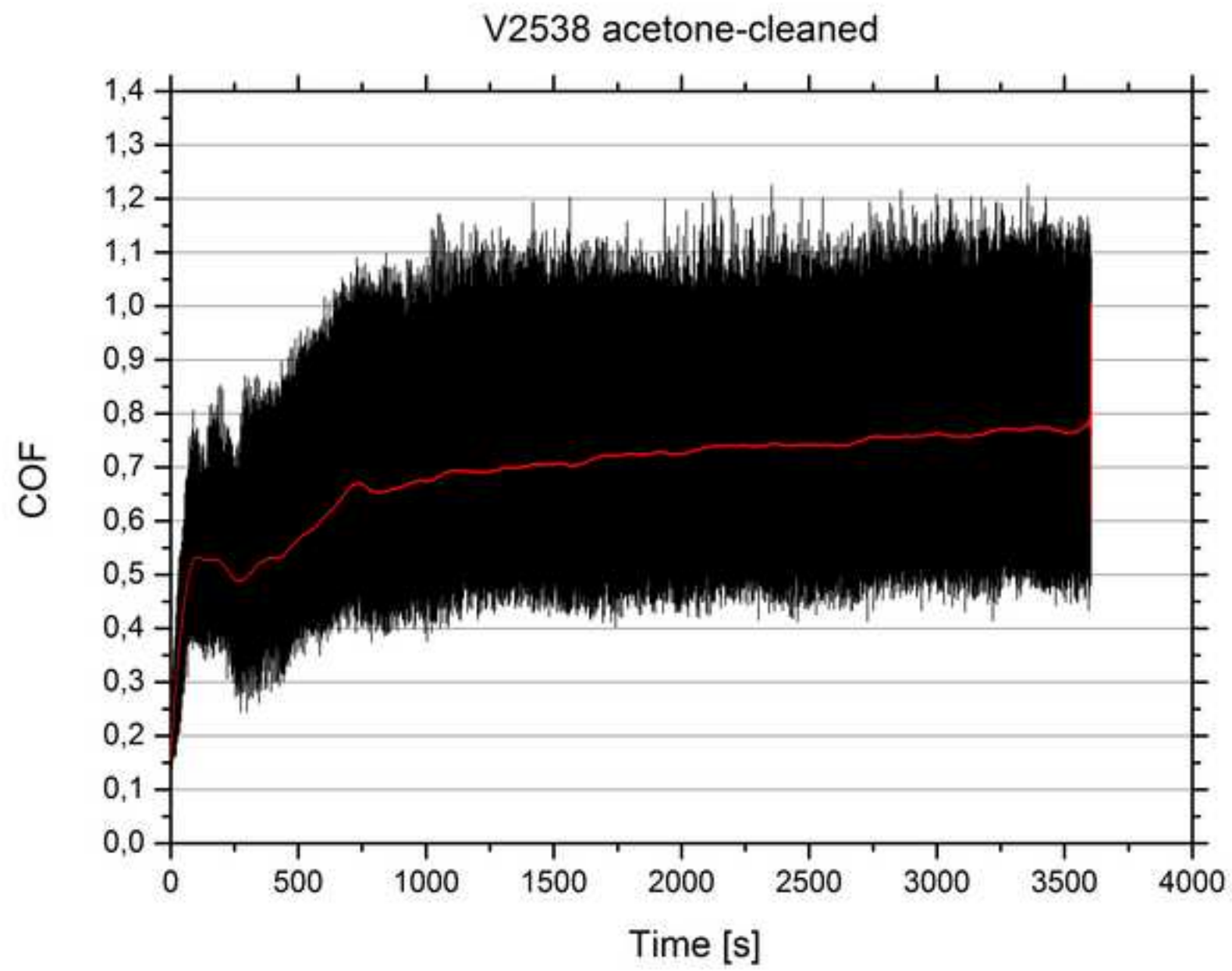


Fig10c

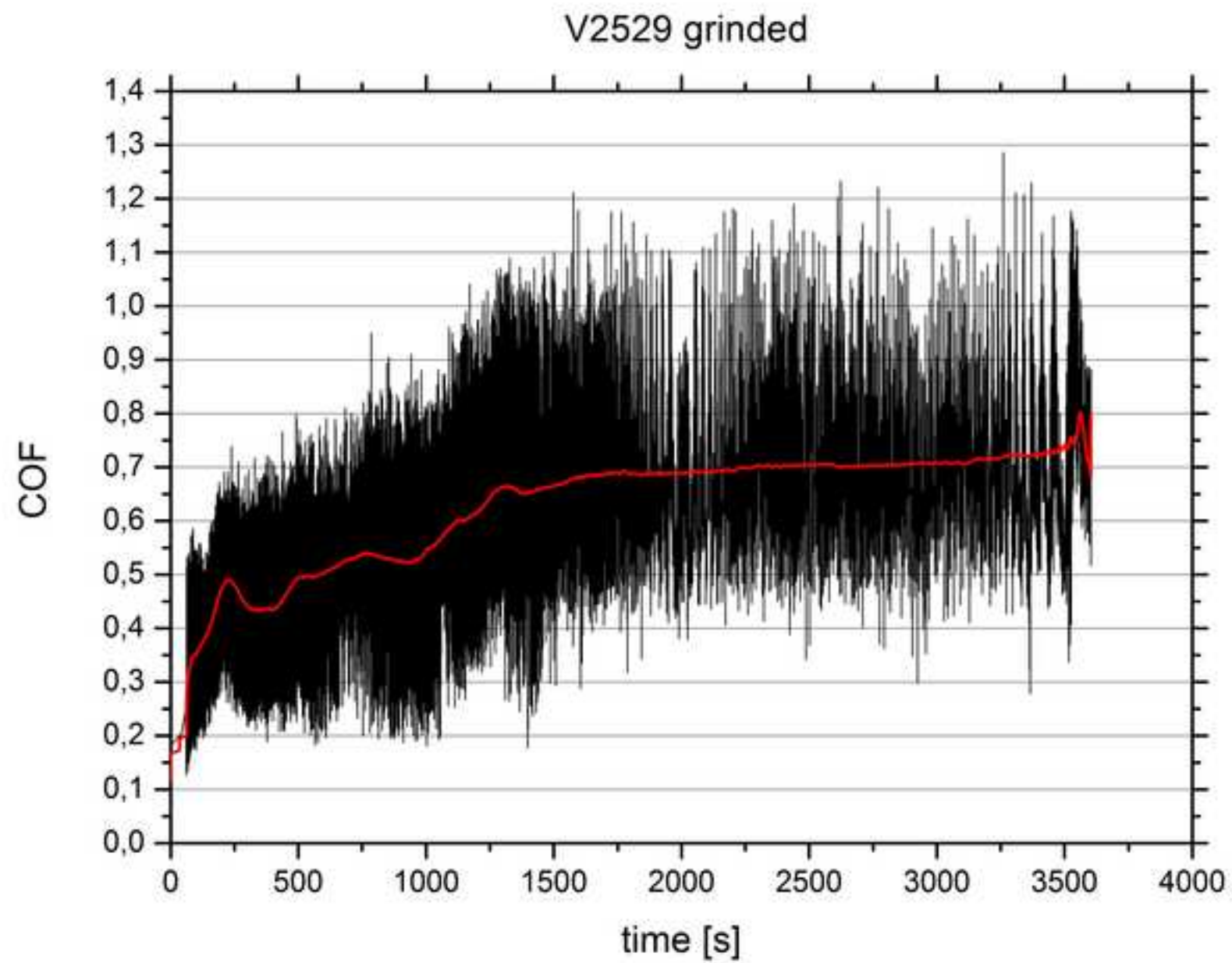




Fig11

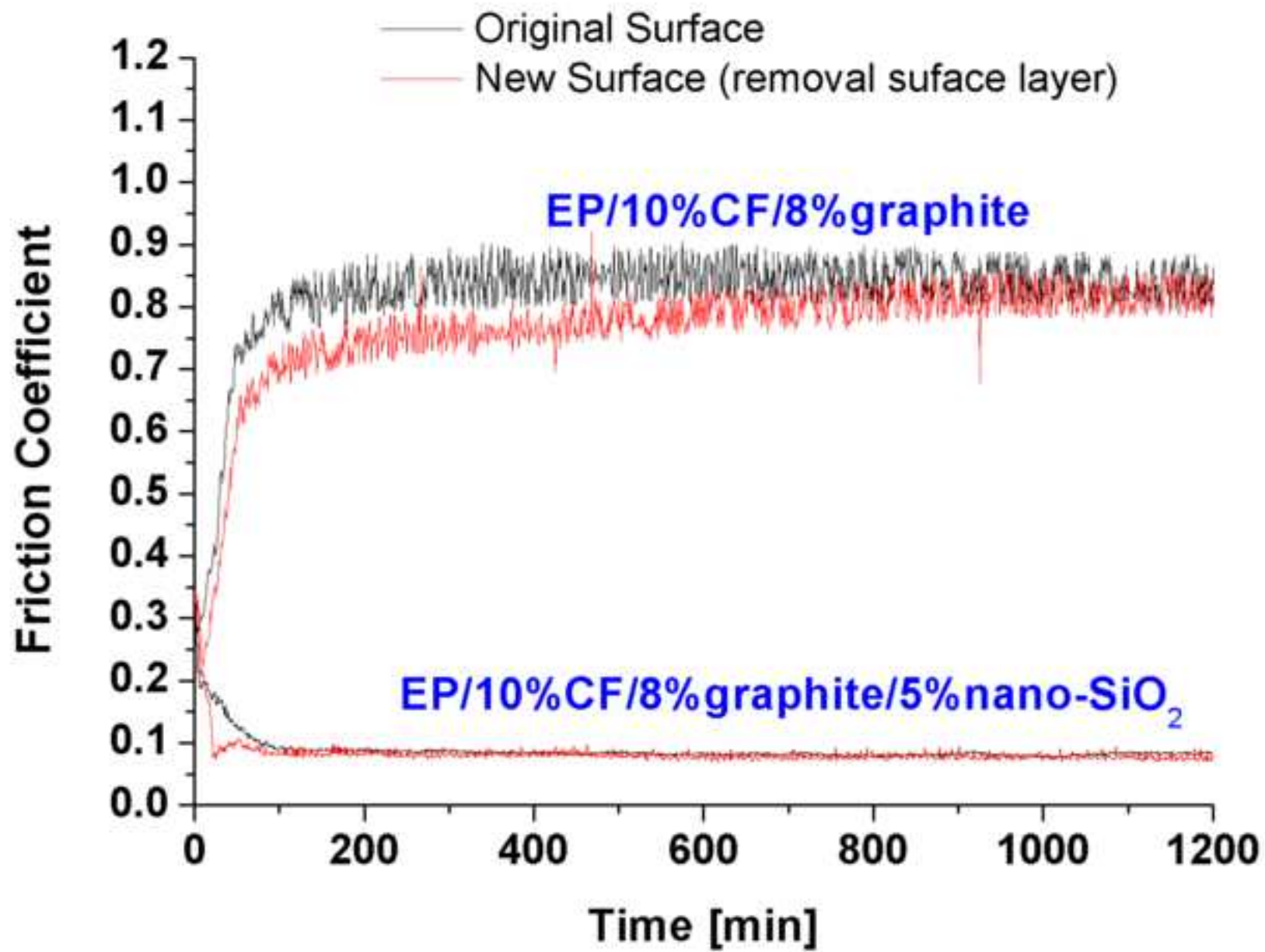


Table 1 Test matrix indicating testing conditions, surface states of 100Cr6 discs and corresponding characterization results

Pin material		100Cr6 pin	Composite H <sup>1</sup>	Composite C <sup>2</sup>	Composite C <sup>2</sup>
Testing conditions	Prior to testing	$F_N=20\text{ N}$ , $v=0.05\text{ m/s}$	$p_v = 3\text{ MPa}\cdot 1\text{ m/s}$	$p_v = 1\text{ MPa}\cdot 1\text{ m/s}$	$p_v = 3\text{ MPa}\cdot 1\text{ m/s}$
Test duration		60 min	1200 min	1200 min	1200 min
Original surface	RS (Fig.1a)	Tribotest (Fig.10a)	Tribotest (Fig.11)	Tribotest [3] X-TEM (Fig.7)	Tribotest (Fig.11)
Acetone-cleaned	RS (Fig.2a) X-TEM (Fig.9)	Tribotest (Fig.10b)	RS (Fig.4b)		
Toluene-cleaned	SEM/EDS (Fig.6)				
After removal of 50 $\mu\text{m}$ thick surface layer	RS (Fig.2b,c)	Tribotest (Fig.10c)	Tribotest (Fig.11) X-TEM (Fig.8)		Tribotest (Fig.11) X-TEM to be publ.

<sup>1</sup> H: Hybrid composite with the composition: EP/10%SCF/8%graphite/5%nano-SiO<sub>2</sub>

<sup>2</sup> C: Conventional Composite with the composition: EP/10%SCF/8%graphite